



HAL
open science

High-resolution Magic-angle Spinning (HR-MAS) NMR Spectroscopy

Alan Wong, Covadonga Lucas-Torres

► **To cite this version:**

Alan Wong, Covadonga Lucas-Torres. High-resolution Magic-angle Spinning (HR-MAS) NMR Spectroscopy. Hector C. Keun. NMR-based Metabolomics, Chapter 5, The Royal Society of Chemistry, pp.133-150, 2018, 978-1-84973-643-5. 10.1039/9781782627937-00133 . cea-01686788

HAL Id: cea-01686788

<https://cea.hal.science/cea-01686788>

Submitted on 18 Jan 2018

HAL is a multi-disciplinary open access archive for the deposit and dissemination of scientific research documents, whether they are published or not. The documents may come from teaching and research institutions in France or abroad, or from public or private research centers.

L'archive ouverte pluridisciplinaire **HAL**, est destinée au dépôt et à la diffusion de documents scientifiques de niveau recherche, publiés ou non, émanant des établissements d'enseignement et de recherche français ou étrangers, des laboratoires publics ou privés.

High-resolution Magic-angle Spinning (HR-MAS) NMR Spectroscopy

ALAN WONG* AND COVADONGA LUCAS-TORRES

NIMBE, CEA, CNRS, Université Paris-Saclay, CEA Saclay, 91191 Gif-sur-Yvette, France

*E-mail: alan.wong@cea.fr

5.1 Introduction

Today, numerous analytical tools are available for metabolomics research;¹ among them, high-resolution ¹H liquid-state NMR spectroscopy offers a quantitative, non-destructive high-throughput method for rapid analysis of biospecimens. Therefore, ¹H liquid-state NMR is widely used and is considered a convenient screening tool to discriminate between specimens of different biological origin.^{2,3} One reason for this success is that in liquid-state NMR the samples are homogeneous (*e.g.*, biofluids), permitting the acquisition of sharp signals (up to 0.001 ppm) for rich metabolic screening. Conversely, semisolid samples like tissue biopsies, whole cells and organisms are heterogeneous in nature and give broad NMR lines that hamper any precise and detailed metabolic investigation. This broadening is caused by the variation of the magnetic susceptibility in intercellular and intracellular boundaries.^{4,5} However, in the early-mid 1990s an NMR technique emerged called high-resolution magic-angle spinning (HR-MAS) that extended the

NMR applications to heterogeneous samples. Essentially, HR-MAS combines two highly successful NMR techniques: the ‘high-resolution’ for liquids and the ‘line-narrowing’ for solids. Basically, HR-MAS averages the magnetic susceptibility gradient and the residual dipolar coupling inherent in heterogeneous samples. This results in NMR spectra of semisolids with a spectral resolution on a par with liquid-state NMR spectroscopy.

The significant technological advancements in the design of HR-MAS probes have led to several commercial probes: HR-MAS by Bruker BioSpin Corporation, FGMAS by JEOL Inc., HR-MAS MAG by Doty Scientific Inc., and Nano Probe by Agilent Technologies. These developments have enabled a wide spectrum of applications, ranging from materials to medical science. In particular, HR-MAS in clinical research is now entering an exciting period, where research scientists and medical doctors are working together to implement a clinical HR-MAS NMR analytical platform for real-time metabolic screening of surgical human biopsies.^{6,7}

There are numerous journal reviews, books and chapters dedicated to HR-MAS NMR spectroscopy; to list just a few, applications to cancer research,^{8–12} food science,^{13,14} cellular science,¹⁵ material science¹⁶ and to science in general^{17–19} are well documented. Clearly, this wide spectrum of applications highlights the great utility of HR-MAS. Literature on the fundamental principles and practical aspects of HR-MAS,^{20,21} and the drawbacks of HR-MAS in metabolomics analysis, is also available.²² This chapter, meant for general readers, outlines the basic principles of HR-MAS and highlights a few noteworthy MAS-based technologies and methodologies that could further advance NMR technology for metabolomics research.

5.2 HR-MAS Basic Concepts

This section briefly describes the sources of line broadening in heterogeneous samples and the line-narrowing techniques used to obtain high-quality NMR spectra for metabolomics studies. Readers can find a more comprehensive description in various books^{23,24} and journal articles.^{25,26}

5.2.1 Magnetic Susceptibility Broadening

In NMR, the effective magnetic field B induced in a sample can be expressed as:

$$B = \mu_0 H_0 + M, \quad (5.1)$$

where H_0 is the external magnetic field, μ_0 is the permeability of free space ($4\pi \times 10^{-7}$ H A⁻¹), and M is the sample magnetization (or magnetic dipole moment) per unit volume. If the magnetic susceptibility of the sample is isotropic, then M can be defined as χB_0 , where χ is a scalar component of the

susceptibility, and $B_0 = \mu_0 H_0$ is the magnetic field induction. Thus, B can be defined as:

$$B = \mu_0 H_0 (1 + \chi) = \mu H_0, \quad (5.2)$$

where $\mu = \mu_0(1 + \chi)$ is the permeability of the sample. From the above equations, the effective field B experienced in a sample depends directly on the susceptibility factor χ , which arises from the local dipole moment M . For example, if a sample is immersed in a homogeneous liquid, the susceptibility of the liquid medium induces an additional homogeneous magnetic field in the sample that results in a shift of the sample NMR signals. Consider the simple case of lipids in muscle tissues, which consist of two distinct lipid compartments: one intra-myocellular and one extra-myocellular. As a result, the related spectrum contains two distinct ^1H NMR signals with a chemical shift difference of about 0.2 ppm, which is attributed to the different susceptibility between the two lipid compartments.²⁷ However, metabolites in tissues are usually immersed in complex heterogeneous media with multiple different cellular boundaries, each of which has a different susceptibility. As a result, a magnetic field gradient ΔB is induced on the metabolites, resulting in a chemical shift gradient and thus in broad ^1H NMR signals.

The magnitude of the susceptibility broadening can be estimated by determining the induced dipolar magnetic field. Consider a dipolar magnetic moment m in a spherical volume (Figure 5.1a) with radius a and permeability $\mu_i = 1 + \chi_i$; and a point P located at distance R from the magnetic moment m and situated in a medium with permeability $\mu_e = 1 + \chi_e$.

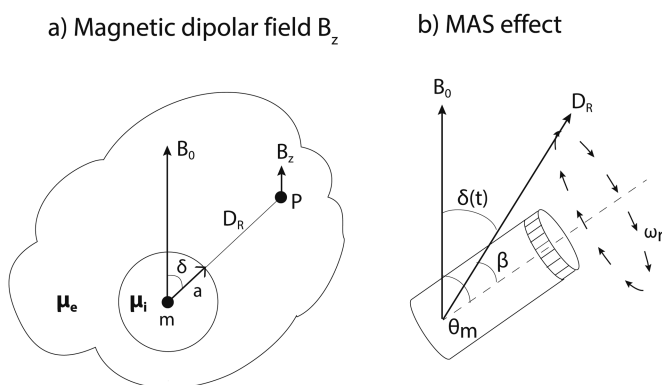


Figure 5.1 (a) The magnetic dipolar field B_z at point P of a sample induced by a magnetic moment m under the external magnetic field B_0 . δ is the angle between B_0 and the dipolar vector D_R , which depends on a distance R from m . (b) The MAS effect on the dipolar interaction, where δ becomes a time-dependent component with magic-angle θ_m and β angle between the rotation axis and D_R [eqn (5.4)].

At the point P, the magnetic moment m generates a dipolar magnetic field B_z . The magnitude of the induced B_z field essentially causes the shift of the signal—in other words line broadening—and can be estimated with the following equation:

$$B_z = -\frac{\Delta\chi}{3} \frac{a^3}{R^3} B_0 (3 \cos^2 \delta - 1) \quad (5.3)$$

where $\Delta\chi$ is the difference in susceptibility between two magnetic volumes $\chi_e - \chi_i$, and δ is the angle between B_0 and the dipolar vector D_R . As can be seen in eqn (5.3), B_z varies with the susceptibility difference ($\Delta\chi$), and the position (distance $1/R^3$ and angle δ). Let us consider a very simple heterogeneous sample—water medium containing an air bubble. The susceptibility of water is 9×10^{-6} , and near zero for the air bubble. In this case, the ^1H signal of the water molecules at the boundaries of the air bubble ($R = a$, Figure 5.1a) is shifted by at most 6 ppm depending on δ . Since this shift decreases with the increasing distance R (*i.e.*, weaker dipolar field), the water molecules around the air bubble give a broad signal caused by the different dipolar fields between the individual water molecule and the air bubble. The same effect, but with different magnitude, is found in the case of metabolites located near air bubbles or cellular structures such as cell membranes.

The ^1H NMR spectra of brain tissues have relatively narrow signals compared to other tissues because the brain metabolites are characterized by fast molecular tumbling, which partially averages the susceptibility effect described above. This is why most static NMR studies – including *in vivo* MRS – on semisolid biosamples have been carried out on brain tissues.^{28,29} To extend NMR-based metabolomics studies to other heterogeneous specimens like biotissues, whole cells and organisms, one has to apply a line-narrowing NMR technique called MAS. This is a commonly used technique in solid-state NMR spectroscopy.

5.2.2 Magic-angle Spinning

As described in the previous section, the susceptibility broadening is caused by the dipolar magnetic field B_z , which varies with the susceptibility $\Delta\chi$, the distance R , and angle δ between the external field B_0 and the dipolar vector D_R [eqn (5.3) and Figure 5.1a]. The angle contribution can be eliminated by spinning the sample at an angle $\theta_m = \cos^{-1}\left(\frac{1}{\sqrt{3}}\right) = 54.74^\circ$ relative to B_0 . This sample-spinning technique was introduced by Andrew³⁰ and Lowe³¹ in 1959, and is known as MAS.

Since the sample rotates in a MAS experiment, δ becomes a time-dependent component and is given by:

$$\cos \delta(t) = \cos \beta \cos \theta_m + \sin \beta \sin \theta_m \cos(\phi(t)) \quad (5.4)$$

where β is the angle between the rotation axis and the dipolar vector (Figure 5.1b). Upon inserting the time-dependent $\delta(t)$ term into eqn (5.3), the effective dipole field inside the spinning sample is:

$$B_z = \mu_0 \frac{m}{2R^3} \left\{ \begin{array}{l} (3\cos^2\beta - 1)(3\cos^2\theta_m - 1) + \\ 3\sin 2\beta \sin 2\theta_m \cos(\omega_r t + \phi) + \\ 3\sin^2\beta \sin^2\theta_m \cos(2(\omega_r t + \phi)) \end{array} \right\} \quad (5.5)$$

where ω_r is the sample-spinning frequency and ϕ is the time-dependent azimuth angle. When $\theta_m = 54.74^\circ$ (*i.e.*, during a MAS experiment), the first term in eqn (5.5) becomes zero, leaving the second and third terms. These terms generate signals called spinning sidebands, which occur at multiple of the spinning frequency ω_r and the amplitude of which depends on the line-width of the signal in non-spinning condition *i.e.*, $\omega_r = 0$. Subsequently, MAS eliminates the susceptibility broadening and results in an isotropic signal at a chemical shift that depends on the nuclear spin chemical shift interaction. To illustrate the substantial effect that MAS can have on the resolution of a spectrum, Figure 5.2 shows the ^1H NMR spectra of a tissue sample acquired with and without MAS.

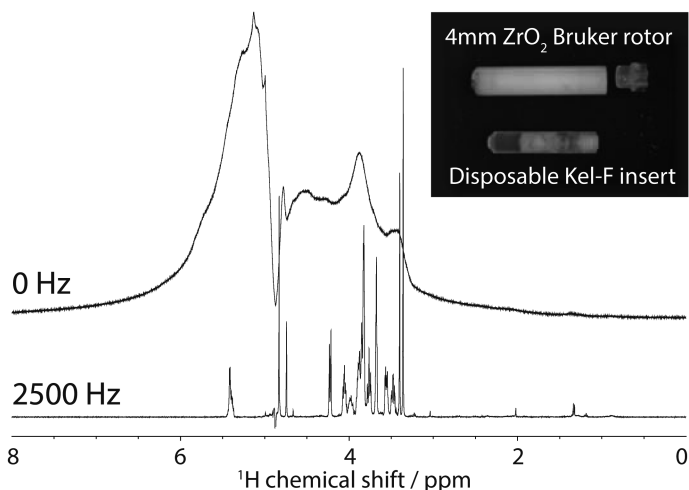


Figure 5.2 ^1H HR-MAS spectra of 10 mg rat brain tissue. The NMR spectra were recorded with a t_2 -cpmg experiment at 500 MHz at 285 K under different MAS conditions: (top) under a non-sample-spinning condition at 0 Hz, and (bottom) at a sample-spinning of 2500 Hz. The tissue was packed inside a standard Bruker disposable Kel-F insert, which is used to enhance the sampling throughput and spectral repeatability.

5.3 Hardware and Practical Considerations

In HR-MAS, the sample is packed inside a spinning rotor, which in turn is placed inside a detection coil. The susceptibility variations between rotor and sample, and within the sample, are not critical since they all average to zero under MAS condition, providing the susceptibilities are isotropic. The residual line broadening in HR-MAS NMR spectra is thus caused by sources that are independent from MAS. One possible source is the magnetic field induced by the stationary (non-spinning) components of the NMR probe that are in close proximity to the sample. This field can perturb the dipolar field in the sample—even if the sample is under MAS conditions—and compromise the spectral quality.

Another possible source of broadening is the presence of local temperature gradients inside the sample, which can originate from spinning, high radiofrequency or electric field. Since in certain cases chemical shifts are temperature-dependent, a temperature gradient in the sample can severely broaden the NMR lines. To minimize the contribution from the NMR probe and temperature gradients, carefully designed HR-MAS probes should be implemented.

5.3.1 Magnetic Susceptibility Components

When designing a HR-MAS probe, one important criterion is to minimize the magnetic dipolar field perturbations B_z in close proximity to the sample. These field perturbations can originate from non-spinning probe components, such as the ceramic MAS stator, the chip capacitors, the wire of the detection coil, the air tubes, the optical devices and the adhesives. Hence, these stationary components must be placed apart from the sample or made of materials with a magnetic susceptibility similar to that of the sample (*i.e.*, water in most cases). For instance, to eliminate the dipolar field perturbation from the detection coil, which is the closest component to the sample, certain probes use coils made with zero-susceptibility wires, like CuNi or CuAl alloy wires.³³

Strategically positioning the stationary chip capacitors with respect to the sample can also reduce the field perturbations, for instance in the case of magic-angle placement of capacitors.³² In a field simulation, it indicates that the dipolar field B_z vanishes at 54.74° with respect to a magnetic moment m . Thus, by symmetrically placing the chip capacitors at near magic-angle with respect to the sample, the field perturbations induced by the capacitors are reduced and the line resolution improved.³²

5.3.2 B_0 Field Correction

Even when a well-designed HR-MAS probe (with minimal local field perturbation to the sample) is inserted inside a NMR magnet, both the sample and probe perturb the B_0 field, leading to a non-homogeneous B_0 field across the

sample, and broadening the NMR signals. To minimize this effect, the B_0 across the sample needs to be corrected—a routine practice in NMR spectroscopy also known as B_0 field shimming. This is done by a set of radio-frequency shims, a series of radiofrequency coils that provide different, but weak, magnetic field profiles. Generally, there are two types of shim coils, the zonal shims (B_{z^1} , B_{z^2} , B_{z^3} ...), which are cylindrically symmetric around the sample axis for reducing on-axis B_0 variations, and the tesseral shims (B_x , B_y , B_{zx} , B_{zy} , B_{xy} , $B_{x^2-y^2}$...), which are used for off-axis B_0 variations.

The shimming of a HR-MAS probe is different than that with a liquid-state NMR probe because of the different orientation of the sample in the two probes. With HR-MAS, the field corrections are applied along the magic-angle axis;^{33,34} moreover, under MAS the inhomogeneity of the B_0 field in the transverse plan is basically averaged to zero, hence no corrections are necessary for the tesseral shims along the magic-angle axis (B_x^{MAS} , B_y^{MAS} , B_{zx}^{MAS} , B_{zy}^{MAS} , $B_{x^2-y^2}^{\text{MAS}}$, B_{xy}^{MAS} ...). Conversely, the inhomogeneity along the magic-angle axis can be corrected by using the zonal shims along the magic angle ($B_{z^1}^{\text{MAS}}$, $B_{z^2}^{\text{MAS}}$, $B_{z^3}^{\text{MAS}}$). This can be done with the conventional shims by adjusting in a linear combination. For example, if the MAS stator lies along the yz plane, the magic-angle zonal shims are:

$$B_{z^1}^{\text{MAS}} = \frac{1}{\sqrt{3}}B_z - \frac{\sqrt{2}}{\sqrt{3}}B_y, \quad (5.6)$$

$$B_{z^2}^{\text{MAS}} = B_{x^2-y^2} - 2\sqrt{2}B_{zy}, \quad (5.7)$$

$$B_{z^3}^{\text{MAS}} = -\frac{2}{3\sqrt{3}}B_{z^3} - \frac{1}{\sqrt{6}}B_{z^2y} + \frac{5}{\sqrt{3}}B_{z(x^2-y^2)} - \frac{5}{3\sqrt{6}}B_y. \quad (5.8)$$

Note that there are no x -directional shims. The exact weighting of these linear combinations is not important under MAS. Often a trial and error shimming procedure is efficient. On the other hand, shimming a MAS sample under non-spinning conditions can be a challenge. In this case, the B_0 inhomogeneity in the transverse plan is not averaged to zero and the magic-angle tesseral shims become significant and must be applied together with the magic-angle zonal shims. Their linear combinations are complex and can be found in ref. 33.

Since different solvents (and samples) can have different susceptibilities (e.g., 9×10^{-6} for H_2O , 8.75×10^{-6} for D_2O , and 7.25×10^{-6} for ethanol), in liquid-state NMR the optimum shim setup can be different. Conversely, an ideal HR-MAS experiment, once optimized the shim setup is efficient for different samples, given that the samples are of the same type and the rotor is at the same position for all experiments. This is because the MAS spinning eliminates the broadening effect generated by the susceptibility gradient inside the spinning sample, whether it is cellular structures, solvents, or even air bubbles or rotors, as long as their susceptibility is isotropic.

5.3.3 B_0 Field Locking

Most HR-MAS probes include a ^2H field-lock system for stabilizing the B_0 in the region around the sample during the data acquisition. Locking the B_0 field is very critical, especially for long acquisitions like multidimensional experiments, because even a small B_0 field drift (parts per billion) can affect the spectral resolution.

The ^2H field-lock system monitors continuously the ^2H signal using a dedicated ^2H -detection channel. Whenever there is a B_0 field drift, the ^2H signal shifts and the ^2H field-lock system automatically adjusts the total field strength to keep the ^2H frequency constant. To ensure that the B_0 field adjustment is within the sample region, the source of the ^2H signal is either mixed within the sample or in close proximity.

5.3.4 Sample Temperature

When a sample is under fast spinning, the air bearing generates a frictional heat on the rotor surface. The frictional heat induces a local temperature gradient inside the rotor. If the ^1H shift of the sample is temperature-dependent, the temperature gradient can broaden the NMR signal. For water, the chemical shift temperature dependence is $11.9 \text{ ppb } ^\circ\text{C}^{-1}$,³⁵ or 6 Hz per degree centigrade at 500 MHz. Therefore, one should avoid using the ^2H -lock for monitoring the D_2O signal level as an indicator of the shimming quality since the automatic shim adjustments can be compromised by the temperature effect and lead to non-optimal shim setup for the metabolite signals. A good practice is to shim directly on a strong metabolite signal, such as the doublets of alanine, glucose or lactate, under a stable sample temperature environment.

It should be noted that besides the friction-induced temperature gradient, radiofrequencies and electric fields can also induce temperature gradients in the sample; therefore, one must also be careful when using high (or lengthy) radiofrequency pulse experiments, or samples with high ionic content.

Two good practices to minimize the local temperature gradient are (i) using cold air (ideally with dry nitrogen gas) for the MAS air bearing and drive, and (ii) keeping the sample temperature constant throughout the measurement even at room temperature.

5.3.5 Pulse-field Gradient

Most of the pulse experiments used in HR-MAS studies of biotissues and cells are derived from liquid-state NMR experiments. This is because the resolution of HR-MAS is on a par with the liquid-state spectra in which the ^1H J -coupling is readily observed. Therefore, standard J -recoupling 2D and 3D experiments, such as COSY, TOCSY and HSQC, can be readily performed under MAS. For these experiments, pulsed-field gradients (PFGs) are an

important feature because gradient pulses can significantly shorten (by up to 25%) the acquisition time. For this reason, most commercial HR-MAS probes include a Z^{MAS} -gradient along the magic-angle axis. This Z^{MAS} -gradient can also be used in a recently implemented ultrafast single-scan 2D experiment (<1 minute) for HR-MAS.³⁶ Another utility of the Z^{MAS} -gradient is that it can offer more efficient water suppression methods³⁷ than that with the conventional radiofrequency pulses. Moreover, with a Z^{MAS} -gradient it is also possible to perform diffusion-related experiments, such as diffusion coefficient measurements and diffusion-edited experiments for improved metabolite identification and annotation.³⁸

Although the Z^{MAS} -gradient in HR-MAS offers good utilities for performing HR-MAS experiments, the capacity of the gradient strength is much lower than that of a dedicated PFG system. For comparison, a conventional Bruker HR-MAS probe provides a gradient of 0.5 T m^{-1} (50 G cm^{-1}) maximum, whereas 30 T m^{-1} (3000 G cm^{-1}) can be reached with a PFG-dedicated system. Strong field gradients are highly desirable for the characterization of molecules with slow diffusion and to perform localized magnetic resonance spectroscopy (MRS), which have found great success in *in vivo* research.^{28,29} For these reasons, Bruker has developed a commercially available PFG system—with three strong orthogonal gradients—that can accommodate a standard Bruker HR-MAS probe for extending the applications of HR-MAS to localized MRS and diffusion-based experiments.³⁹

5.3.6 Pulse Experiments

As mentioned before, most of HR-MAS pulse experiments are adopted from liquid-state NMR—NOESY, CPMG, TOCSY, *J*-resolved and diffusion. Even complex experiments like 3D HCCH-TOCSY and HCCH-COSY have been implemented for HR-MAS.⁴⁰ In standard experiments such as TOCSY, COSY and NOESY, rotor synchronization is generally not important under fast MAS conditions (faster than 2 kHz). However, a few practical aspects should be considered in the case of semisolid heterogeneous samples. For examples, the short transverse relaxation T_2 as compared to liquid-state must be taken into account in the pulse experiments, which can lead to residual dipolar broadening (large proteins) that cannot be averaged to zero even at high MAS frequencies. The spinning effects on the sample must also be considered.

Conversely, rotor synchronization is requisite for certain slow MAS experiments (<1 kHz). For example, the spinning-sideband suppression experiment PASS (Phase Alternated Spinning Sidebands)⁴¹ must be performed under rotor synchronization to completely suppress the spinning-sideband signals. Incidentally, because of the long rotor period ($2\pi/\omega_r$) used under slow MAS, the PASS experiment can also partly be considered a T_2 -filter (similar to a T_2 -edited CPMG experiment) for suppressing the resonances from large molecules that usually mask the metabolite signals and distort the baseline.

5.4 Recent (HR)-MAS Developments Towards NMR-based Metabolomics

5.4.1 *In vivo* Studies

HR-MAS finds success in health and biological sciences mainly for *ex vivo* systems, but only a small number of reports on *in vivo* studies of living organisms. HR-MAS is known to be a non-destructive technique; clearly, with living organisms it is not always the case: can the organisms survive under a spinning condition? How does the spinning affect their vital functionalities?

The first *in vivo* HR-MAS experiment was performed by Tzika and coworkers on the fruit fly, *Drosophila melanogaster*.^{42,43} The authors investigated the metabolic profile variations of injured, aged and immune-deficient flies by ¹H HR-MAS. High-quality ¹H spectra were acquired at 600 MHz, on a single fly and spinning the fly at 2 kHz. The study revealed an increased level of triglycerides in the injured, immune, aged and obese flies that may be indicative of insulin resistance. Although this study has demonstrated the feasibility of HR-MAS metabolic fingerprinting of a whole organism, the obtained ¹H NMR spectra correspond to the metabolic profile of the whole *Drosophila*. More interesting is to obtain metabolic profiles of specific parts and organs of an organism. In this regard, very recently Sarou-Kanian *et al.*⁴⁴ reported a new method—¹H HR-MAS Slice Localized Spectroscopy and HR-MAS Chemical Shift Imaging—to obtain the spatial distribution of metabolites along the anteroposterior axis of the organism. The experiment was acquired on a single living *Drosophila*, using a 3.2 mm MAS probe coupled with a three axes PFG system, at 750 MHz and spinning the fly at 2.6 kHz. The authors successfully obtained individual spectra for the abdomen, thorax and head.

After the successes of Tzika and coworkers with the fruit fly,^{42,43} Bunescu *et al.*⁴⁵ performed *in vivo* metabolic profiling of the aging freshwater cladoceran *Daphnia magna*, and found that the organism survival rate declines steadily with increasing sample-spinning frequency: 84%, 75% and 37% after spinning 20 minutes at 0 Hz, 2 kHz and 3.6 kHz, respectively. This is ascribed to the effect of the centrifugal force on the living organisms, and should be carefully considered when planning *in vivo* HR-MAS experiments and interpreting the *in vivo* results. A good option is applying slow MAS experiments to minimize the centrifugal effect.

5.4.2 Slow MAS Experiments

For heterogeneous biospecimens, sample-spinning frequencies of 2–6 kHz are generally sufficient to obtain high-resolution spectra. In fact, such MAS rates are not required for removing the susceptibility line broadening (see Section 5.2.2) but for suppressing the spinning sidebands within the metabolite spectral region (0–10 ppm in ¹H NMR). A good practice is to have the

spinning sidebands at least 5 ppm apart from the isotropic line *i.e.*, using a spinning frequency of 2 kHz at 400 MHz, and 3 kHz at 600 MHz. This is why, at high magnetic fields, it is generally required to spin the sample at a higher rate. However, as mentioned before, the strong centrifugal force at fast MAS rates can damage the tissue or cell morphologies, alter the metabolic profile,²¹ and eventually compromise the data interpretation. For example, cells in adipocytes were damaged after 2 hours of spinning at 3500 Hz,⁴⁶ visible ruptures in *Caenorhabditis elegans* were observed after 4 hours at 3500 Hz,⁴⁷ and distortion of human brain tumor tissues⁴⁸ and cell lysis⁴⁹ were observed after spinning at 4000 Hz.

The centrifugal force exerted at a given point in the sample is given by:

$$F_c = m\omega_r^2 r \quad (5.9)$$

where m is the sample mass, ω_r is the spinning frequency, and r is the radial distance between the rotation axis and the point. As shown in the equation, F_c increases with both the spinning frequency and sample diameter.

Besides the centrifugal force, sample heating is also a potential drawback of fast MAS as the friction-induced heat reduces the spectral resolution and alters the metabolic activities. Slow MAS reduces the effect of both the centrifugal force and sample heating; however, special pulse sequences are often necessary to suppress the spinning sidebands. Moreover, at slow MAS rates the overall signal intensity is distributed throughout the spinning sidebands, reducing the sensitivity of metabolite detection. Various works have demonstrated that applying the 2D PASS sideband suppression pulse sequence,⁴¹ it is possible to acquire MAS spectra of living bacterial cells⁵⁰ and animal tissues^{51,52} at a spinning speed of only 40 Hz. For even lower spinning (*i.e.*, down to 1 Hz), a more sophisticated pulse experiment is required, the PHase cORRECTed Magic-Angle Turning (PHORMAT).⁵³ The PHORMAT experiment has been demonstrated on rat liver tissues⁵⁴ and proved to be superior to PASS⁵⁵ at ultraslow MAS rates. Combining slow MAS experiments (PASS or PHORMAT) with the use of a small-diameter detection coil—a 700 μm microcoil—Wong and coworkers⁵⁶ were able to further reduce the effect of the centrifugal force [as both ω_r and r contributions in eqn (5.9) are minimized].

At 1 Hz (about 6.3 rotations per second), *in vivo* MAS studies of live animals become possible. Wind and coworkers successfully acquired ^1H NMR spectra with modest spectral resolution of a live mouse spinning at 1.5 Hz.⁵⁷ Later, the same authors demonstrated the capability of *in vivo* localized spectroscopy combining the Localized Magic-Angle Turning (LOCMAT) pulse experiment with a three axes PFG system.⁵⁸ These demonstrative studies opened new perspectives for *in vivo* NMR applications.

Recently, Caldarelli and coworkers^{59,60} demonstrated that high-quality ^1H spectra can be acquired at spinning frequencies of a few hundred hertz without the need for complex sideband suppression pulse sequences. The idea is to reduce the sideband intensities by minimizing the susceptibility

gradient within the sample. To do this, the authors proposed a sample-packing protocol that improves the sample homogeneity by, for instance, eliminating the air bubbles and using symmetrical sample holders (Kel-F sample insert).

For an in-depth description of slow MAS and its applications to biospecimens, readers can refer to ref. 61.

5.4.3 Magic-angle Field Spinning

As mentioned in the previous section, the LOCMAT experiments on a live mouse under ultraslow MAS^{57,58} illustrated the possibility of *in vivo* MAS-based NMR investigations on animal models, and even human subjects. Clearly, spinning a human body at even 1 Hz is not practicable; however, spinning the magnetic field at the magic angle with respect to a living animal or human is possible. The effect of spinning the magnetic field is essentially the same as spinning the sample; it averages the magnetic susceptibility line broadening to zero. Figure 5.3 illustrates the two existing approaches for generating a tilted magnetic field at the magic angle to the subject: (1) using small permanent magnets strategically positioned to set the direction of the magnetic field at the magic angle; and (2) using electromagnet or superconducting magnet through a set of three pairs of orthogonal coils for generating a total field at a specific angle. In both cases, the spinning field can be generated by mechanically rotating the entire unit. In the case of electromagnets, the spinning field can also be obtained by generating time-dependent fields along the three coordinate directions.

In 1968, Bradbury and coworkers⁶² first explored the idea of NMR spectroscopy in rotating magnetic fields but with little success. About 40 years later, Pines and coworkers performed the first successful magic-angle field spinning experiment^{63,64} using electromagnets with three orthogonal

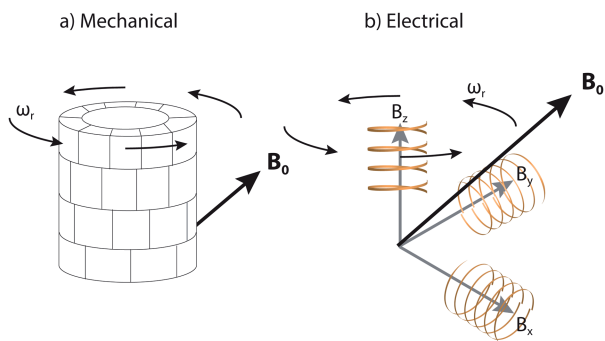


Figure 5.3 The two approaches for creating a tilted magnetic field B_0 oriented at magic-angle with respect to a stationary subject: (a) Mechanically using permanent magnets, and (b) electronically (or superconducting) using three-pairs of orthogonal coils.

Helmholtz pairs generating a rotating field of 0.034 T (1.45 MHz for ^1H). In 2010, Sakellariou and coworkers constructed a prototype of a tilted magnetic field using small and inexpensive permanent cubic magnets.⁶⁵ The design consists of two sets of magnets producing a longitudinal field (at ~ 0.13 T) and a transverse field (at ~ 0.18 T) components and creating a total magnetic field of about 0.22 T that is tilted at an angle of 54.6° with respect to the longitudinal axis of the magnet. In 2013, Iwasa and coworkers developed the first prototype of superconducting magic-angle field magnet.⁶⁶ The magnet is composed of a z-axis 0.866 T solenoid and x-axis 1.225 T dipole operated at 4.2 K. The combined fields produce a 1.5 T field (63.83 MHz for ^1H) at a magic angle with respect to the rotational z-axis. However, the magnet spinning mechanism has yet to be implemented, and there are no spectral data available.

Whether it is a permanent or superconducting magnet, both the stability and homogeneity of the B_0 field are essential for high-resolution NMR spectroscopy (as per the static commercial NMR magnets). If successfully implemented, high spectral quality NMR magic-angle-spinning magnets would find a wide range of new applications, including *in vivo* metabolic investigations with animal and human subjects.

5.4.4 Microscopic Quantity

As NMR is an inherently insensitive technique, HR-MAS studies require large sample volumes, typically 10–20 mg per NMR data. Therefore, HR-MAS can be a real challenge or even impossible when specimens are scarce, like in the case of specific cell types or living organisms, or rare diseased biopsies. Moreover, the investigation of a target cell group can be difficult.

Analyses of small samples (<1 mg) would simplify the sample preparation in case of scarce specimens, and also would make the study of specific specimens possible. One way to increase the mass sensitivity (signal-to-noise per unit mass) is miniaturizing the detection coil for maximizing the radiofrequency field per unit current (B_1/i) and the filling factor (the ratio of the sample volume to the coil detection volume).⁶⁷ Two recent reports showcase the advancements in μ coil technology for liquid-state NMR spectroscopy in biological samples: (1) the design of a micro-NMR diagnostic device for the analysis of human tumor samples,⁶⁸ and (2) the near complete liquid-state NMR assignment of a 68-residue protein using only 6 μl of a 1.4 mM protein solution.⁶⁹

Metabolomics studies that use μ coil detection under MAS conditions are nearly non-existent because assembling a μ coil for sample spinning with high-resolution capability is a real challenge. The current commercial μ MAS probes (0.7 mm Bruker MAS and 0.75 mm JEOL MAS) are designed for solids and provide spectral resolutions of 0.01 ppm, not suitable for metabolic investigations, which require at least 0.002 ppm.

A different approach for the analysis of mass-limited biospecimens is the High-Resolution Magic-Angle Coil Spinning (HR-MACS) technique.^{70,71} In HR-MACS, as with the original MACS experiment,⁷² a secondary tuned

circuit and a simple and robust rotor insert are fit inside a standard MAS sample rotor to convert the MAS probe into a μ MAS probe without any probe modification. Using HR-MACS, Wong and coworkers were able to perform metabolic profiling of whole small organisms (*Caenorhabditis elegans*)⁷³ and intact cells (*Saccharomyces cerevisiae*)⁷⁴ with only 250 μ g of biospecimens (Figure 5.4a). Unfortunately, the effort required for fabricating and operating the HR-MACS μ coil limits the application of HR-MACS to metabolomics research, especially for large-scale sampling studies.

Very recently, Wong and coworkers, together with JEOL Resonance Inc., introduced a high-resolution-capable 1 mm μ MAS probe (denoted as HR- μ MAS)⁷⁵ specifically designed—using a susceptibility-matched MAS stator and coil—for metabolomics studies of scarce specimens <500 μ g. The HR- μ MAS probe, similar to the standard 4 mm HR-MAS probes, integrates a ^2H -locking device for high-resolution acquisition and a temperature regulation unit. It is also capable of stable MAS spinning and high spectral resolution acquisition. Figure 5.4b illustrates the excellent spectra obtained

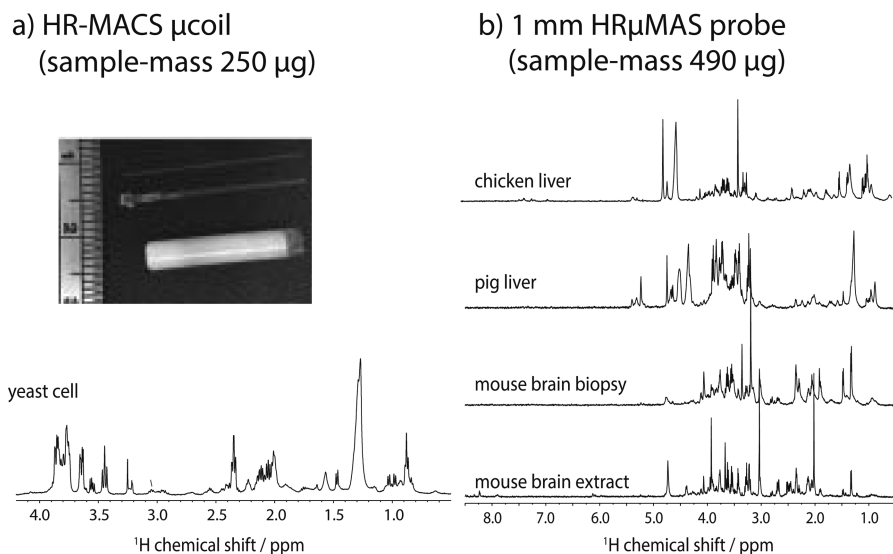


Figure 5.4 Examples of ^1H NMR spectra of microgram specimens acquired from (a) HR-MACS self-resonant μ coil and (b) 1 mm HR- μ MAS probe. In (a), the insert photo displays a hand-wound HR-MACS μ coil with a coil-diameter of 550 μ m, and a Bruker 4 mm ZrO_2 rotor for size comparison. A ^1H HR-MACS NMR spectrum of 250 μ g of intact *Saccharomyces cerevisiae* cells is shown. The spectrum was acquired with a 550 μ m HR-MACS at 500 MHz with a MAS frequency of 300 Hz. In (b), it displays a series of high-quality ^1H NMR spectra of different biospecimens (490 μ g) recorded using a 1 mm HR- μ MAS probe. The spectra were acquired with MAS at 2000 Hz at 600 MHz at 295 K. The total acquisition time for all spectra in (a) and (b) is between 10 and 20 minutes, and the spectral resolution is <0.002 ppm, on a par with the liquid-state NMR standard.

with HR- μ MAS on different biospecimens. Seeing the first promising results, the HR- μ MAS NMR probe will likely become a routine analytical tool for metabolomics.

5.5 Concluding Remarks

After two decades of development and exploration of the HR-MAS technique for NMR-based metabolomics research, the early challenge of obtaining high spectral resolution data and developing applications for metabolomics have been fully addressed. Subsequently, HR-MAS has now become an invaluable NMR spectroscopic technique that is routinely applied in biological and medical science for obtaining crucial metabolic information from *ex vivo* intact specimens, and relating them to *in vivo* systems.

Despite the tremendous progress made in HR-MAS NMR for metabolomics, the technique has yet to become a reliable platform for *in vivo* systems. With the continuous development in the HR-MAS technology, we believe that *in vivo* HR-MAS will one day become a vital screening tool for metabolomics research. Hopefully, this introductory chapter will encourage scientists in all fields—engineering, physics or biology—to explore the current (or new) MAS technologies and continue the advancement of HR-MAS NMR-based metabolomics.

Acknowledgements

I would like to thank the French National Research Agency (ANR-12-JSV5-0005) and Nanosciences et Innovation pour les Matériaux, la Biomédecine et l'Énergie (NIMBE) at CEA Saclay for their support, and Dr Fabrizia Poli for her valuable inputs on the chapter.

References

1. W. B. Dunn and D. I. Ellis, *Trends Anal. Chem.*, 2005, **24**, 285.
2. J. C. Lindon, E. Holmes and J. K. Nicholson, *Anal. Chem.*, 2003, **75**, 384A.
3. N. V. Reo, *Drug Chem. Toxicol.*, 2002, **25**, 375.
4. F. Adebodun and J. F. M. Post, *NMR Biomed.*, 1993, **6**, 125.
5. P. Weybright, K. Millis, N. Campbell, D. G. Cory and S. Singer, *Magn. Reson. Med.*, 1998, **39**, 337.
6. J. K. Nicholson, E. Holmes, J. M. Kinross, A. W. Darzi, Z. Takats and J. C. Lindon, *Nature*, 2012, **491**, 384.
7. M. Piotto, F. M. Moussallieh, A. Neuville, J. P. Bellocq, K. Elbayed and I. J. Namer, *J. Med. Case Rep.*, 2012, **6**, 22.
8. H. Keun, *Methods Enzymol.*, 2014, **543**, 297.
9. E. M. Defeo and L. L. Cheng, *Technol. Cancer Res. Treat.*, 2010, **9**, 381.
10. E. M. Defeo and L. L. Cheng, *NMR Biomed.*, 2014, **27**, 90.
11. B. Sitter, T. F. Bathen, M. B. Tessem and I. S. Gribbestad, *Prog. Nucl. Magn. Reson. Spectrosc.*, 2009, **54**, 239.

12. S. Moestue, B. Sitter, T. F. Bathen, M.-B. Tessem and I. S. Gribbestad, *Curr. Top. Med. Chem.*, 2011, **11**, 2.
13. M. Valentini, M. Ritota, C. Cafiero, S. Cozzolino, L. Leita and P. Sequi, *Magn. Reson. Chem.*, 2011, **49**, S121.
14. A. M. Gil and I. F. Duarte, *Modern Magn. Reson.*, 2006, 1765.
15. W. Li, *Analyst*, 2006, **131**, 777.
16. T. M. Alam and J. E. Jenkins, in *Advanced Aspects of Spectroscopy*, ed. M. A. Farrukh, InTech, 2012, ch. 10, pp. 279–306.
17. W. P. Power, *Annu. Rep. NMR Spectrosc.*, 2003, **51**, 261.
18. W. P. Power, *Annu. Rep. NMR Spectrosc.*, 2010, **72**, 111.
19. J. C. Lindon, O. P. Beckonert, E. Holmes and J. K. Nicholson, *Prog. Nucl. Magn. Reson. Spectrosc.*, 2009, **55**, 79.
20. O. Beckonert, M. Coen, H. C. Keun, Y. Wang, T. M. D. Ebbels, E. Holmes, J. C. Lindon and J. K. Nicholson, *Nat. Protoc.*, 2010, **5**, 1019.
21. J.-H. Chen and S. Singer, in *The Handbook of Metabonomics and Metabolomics*, ed. J. C. Lindon, J. K. Nicholson and E. Holmes, Elsevier, Oxford, 2007, ch. 4, pp. 113–147.
22. V. Esteve, B. Martinez-Granados and M. Martinez-Bisbal, *Front. Chem.*, 2014, **2**, 33.
23. D. L. VanderHart, in *Encyclopedia of Magnetic Resonance*, ed. D. M. Grant and R. K. Harris, John Wiley & Sons, New York, 1996, pp. 2938–2946.
24. A. Abragam, *The Principles of Nuclear Magnetism*, Clarendon Press, 1961.
25. A. N. Garroway, *J. Magn. Reson.*, 1982, **49**, 168.
26. F. D. Doty, G. Entzminger and Y. A. Yang, *Conc. Magn. Reson.*, 1998, **10**, 133.
27. F. Schick, B. Eismann, W.-I. Jung, H. Bongers, M. Bunse and O. Lutz, *Magn. Reson. Med.*, 1993, **29**, 158.
28. M. Van der Graaf, *Eur. Biophys. J.*, 2010, **39**, 527.
29. S. Ramadan, A. Lin and P. Stanwell, *NMR Biomed.*, 2013, **26**, 1630.
30. E. R. Andrew and R. G. Eades, *Nature*, 1959, **183**, 1802.
31. I. J. Lowe, *Phys. Rev. Lett.*, 1959, **2**, 285.
32. F. D. Doty, G. Entzminger and Y. A. Yang, *Concepts Magn. Reson.*, 1998, **10**, 239.
33. A. Sodickson and D. G. Cory, *J. Magn. Reson.*, 1997, **128**, 87.
34. M. Piotto, K. Elbayed, J.-M. Wieruszkeski and G. Lippens, *J. Magn. Reson.*, 2005, **173**, 84.
35. D. S. Wishart, C. G. Bigam, J. Yao, F. Abildgaard, H. J. Dyson, E. Oldfield, J. L. Markley and B. D. Sykes, *J. Biomol. NMR*, 1995, **6**, 135.
36. M. Andre, M. Piotto, S. Caldarelli and J.-N. Dumez, *Analyst*, 2015, **140**, 3942.
37. M. Piotto, V. Saudek and V. Sklenář, *J. Biomol. NMR*, 1992, **2**, 661.
38. S. Viel, F. Ziarelli and S. Caldarelli, *Proc. Natl. Acad. Sci. U. S. A.*, 2003, **100**, 9696.
39. A. Pampel, F. Engelke, D. Groß, T. Oerther and K. Zick, *Bruker SpinReport*, 2006, vol. 157/158, p. 26.
40. W. Li, R. E. Lee, R. E. Lee and J. Li, *Anal. Chem.*, 2005, **77**, 5785.

41. O. N. Antzutkin, Z. Song, X. Feng and M. H. Levitt, *J. Chem. Phys.*, 1994, **100**, 130.
42. V. Righi, Y. Apidianakis, D. Mintzopoulos, L. Astrakas, L. G. Rahme and A. A. Tzika, *Int. J. Mol. Med.*, 2010, **26**, 175.
43. V. Righi, Y. Apidianakis, L. G. Rahme and A. A. Tzika, *J. Visualized Exp.*, 2010, **38**, e1710.
44. V. Sarou-Kanian, N. Joudiou, F. Louat, M. Yon, F. Szeremeta, S. Mème, D. Massiot, M. Decoville, F. Fayon and J.-C. Beloeil, *Sci. Rep.*, 2015, **5**, 9872.
45. A. Bunescu, J. Garric, B. Vollat, E. Canet-Soulas, D. Graveron-Demilly and F. Fauvelle, *Mol. BioSyst.*, 2010, **6**, 121.
46. P. Weybright, K. Millis, N. Campbell, D. G. Cory and S. Singer, *Magn. Reson. Med.*, 1998, **39**, 337.
47. B. J. Blaise, J. Giacomotto, M. N. Triba, P. Toulhoat, M. Piotto, L. Emsley, L. Ségalat, M. E. Dumas and B. Elena, *J. Proteome Res.*, 2009, **8**, 2542.
48. M. C. Martinez-Bisbal, V. Esteve, B. Martinez-Granado and B. Celda, *J. Biomed. Biotech.*, 2011, 763684.
49. S. Aime, E. Bruno, C. Cabella, S. Sebastiano, G. Digilio and V. Mainero, *Magn. Reson. Med.*, 2005, **54**, 1547.
50. J. Z. Hu, R. A. Wind, J. McLean, Y. A. Gorby, C. T. Resch and J. K. Fredrickson, *Spectroscopy*, 2004, **19**, 98.
51. H. C. Bertram, J. Z. Hu, D. N. Rommereim, R. A. Wind and H. J. Andersen, *J. Agric. Food Chem.*, 2004, **52**, 2681.
52. H. C. Bertram, H. J. Jakobsen and O. B. Nielsen, *J. Agric. Food Chem.*, 2005, **53**, 3229.
53. J. Z. Hu, W. Wang, F. Liu, M. S. Solum, D. W. Alderman, R. J. Pugmire and D. M. Grant, *J. Magn. Reson., Ser. A*, 1995, **113**, 210.
54. J. Z. Hu, D. N. Rommereim and R. A. Wind, *Magn. Reson. Med.*, 2002, **47**, 829.
55. J. Z. Hu and R. A. Wind, *J. Magn. Reson.*, 2002, **159**, 92.
56. A. Wong, P. M. Aguiar and D. Sakellariou, *Magn. Reson. Med.*, 2010, **63**, 269.
57. R. A. Wind, J. Z. Hu and D. N. Rommereim, *Magn. Reson. Med.*, 2003, **50**, 1113.
58. R. A. Wind, J. Z. Hu and P. D. Majors, *Magn. Reson. Med.*, 2006, **55**, 41.
59. M. Renault, L. Shintu, M. Piotto and S. Caldarelli, *Sci. Rep.*, 2013, **3**, 3349.
60. M. Andre, J.-N. Dumez, L. Rezig, L. Shintu, M. Piotto and S. Caldarelli, *Anal. Chem.*, 2014, **86**, 10749.
61. R. A. Wind and J. Z. Hu, *Prog. Nucl. Magn. Reson. Spectrosc.*, 2006, **49**, 207.
62. A. Bradbury, R. G. Eades and J. G. McCarten, *Phys. Lett.*, 1968, **26A**, 405.
63. C. A. Meriles, D. Sakellariou, A. Moule, M. Goldman, T. F. Budinger and A. Pines, *J. Magn. Reson.*, 2004, **169**, 13.
64. D. Sakellariou, C. A. Meriles, R. W. Martin and A. Pines, *Magn. Reson. Imaging*, 2005, **23**, 295.
65. D. Sakellariou, C. Hugon, A. Guiga, G. Aubert, S. Cazaux and P. Hardy, *Magn. Reson. Chem.*, 2010, **48**, 903.

66. J. Voccio, S. Hahn, D. K. Park, J. Ling, Y. Kim, J. Bascuñán and Y. Iwasa, *IEEE Trans. Appl. Supercond.*, 2013, **23**, 4300804.
67. D. I. Hoult and R. E. Richards, *J. Magn. Reson.*, 1976, **24**, 71.
68. J. B. Haun, C. M. Castro, R. Wang, V. M. Peterson, B. S. Marinelli, H. Lee and R. Weissleder, *Sci. Transl. Med.*, 2011, **3**, 71ra16.
69. J. M. Aramini, P. Rossi, C. Anklin, R. Xiao and G. T. Montelione, *Nat. Methods*, 2007, **4**, 491.
70. A. Wong, B. Jiménez, X. Li, E. Holmes, J. K. Nicholson, J. C. Lindon and D. Sakellariou, *Anal. Chem.*, 2012, **84**, 3843.
71. A. Wong, X. Li and D. Sakellariou, *Anal. Chem.*, 2013, **85**, 2021.
72. D. Sakellariou, G. Le Goff and J.-F. Jacquinot, *Nature*, 2007, **447**, 694.
73. A. Wong, X. Li, L. Molin, F. Solari, B. Elena-Herrmann and D. Sakellariou, *Anal. Chem.*, 2014, **86**, 6064.
74. A. Wong, C. Boutin and P. M. Aguiar, *Front. Chem.*, 2014, **2**, 38.
75. Y. Nishiyama, Y. Endo, T. Nemoto, A.-K. Bouzier-Sore and A. Wong, *Analyst*, 2015, **140**, 8097.